Author/s:
Roy, A;Chow, S

Title:
Plate anchor capacity estimation through CPT tip resistance in sand

Date:
2022-06-15

Citation:
Roy, A. & Chow, S. (2022). Plate anchor capacity estimation through CPT tip resistance in sand. Gottardi, G (Ed.) Tonni, L (Ed.) Proceedings of the 5th International Symposium on Cone Penetration Testing 2022, pp.1077-1082. Taylor and Francis group. https://doi.org/10.1201/9781003308829-163.

Persistent Link:
https://hdl.handle.net/11343/311316

Cone Penetration Testing 2022 – Gottardi & Tonni (eds)

Plate anchor capacity estimation through CPT tip resistance in sand

A. Roy & S.H. Chow
Department of Infrastructure Engineering, the University of Melbourne, Australia

ABSTRACT: Reliable estimation of plate anchor uplift capacity in sand through analytical and empirical equations is often complicated due to uncertainties in estimation of soil properties required in the equations. In order to address this uncertainty, this study proposes a correlation to estimate plate anchor vertical uplift capacity in sand based on cone tip resistance measured from cone penetrometer tests (CPT). The correlation was established using a database of reported centrifuge experiments on circular, rectangular and strip anchors in loose and dense silica sand at various embedment depths and *g*-levels, along with the corresponding centrifuge CPTs performed in the same testing boxes. The centrifuge cone tip resistances were also depth-corrected to remove the effect of shallow embedment. Through regression analyses, the correlation between plate anchor capacity and cone tip resistance in dimensionless form was developed, with different coefficients fitted for circular, rectangular and strip anchors respectively.

1 INTRODUCTION

Plate anchors are routinely used onshore as foundations for structures subjected to high uplift or lateral loads. With a recent global thrust in harnessing energy from cleaner renewable energy sources, plate anchors are also likely to find increased application in mooring offshore renewable energy devices owing to their cost- and capacity-effectiveness relative to other anchors and piles. Such renewable energy devices are likely to be located in much shallower water where the seabeds of interest include coarser-grained deposits. Hence, reliable estimation of plate anchor uplift capacity in coarser-grained soils will be of interest for geotechnical practitioners.

One of the most widely used soil exploration methods in coarser-grained offshore deposits is cone penetration tests (CPT). As undisturbed core sample collection for coarser-grained soils requires specialised equipment and becomes expensive for offshore sites, CPT data is often the only source of geotechnical information available during the early planning stages for offshore projects. Considering that behaviour in sands is highly dependent on initial fabric, stress levels and relative density (R_D) (Been et al. 1991, Gajo & Wood 1999), a continuous CPT profile can macroscopically capture such effects with respect to the change in soil stratigraphy. As compared to a traditional 'operational' friction angle (φ) based approach, there is great value in direct application of cone tip resistance (q_c) profiles in design approaches, because it will significantly improve reliability in prediction by eliminating uncertainties in estimation of a back-analysed φ. Such q_c based design approaches have been reported for bearing capacity problems on footings and spudcans (Lee & Salgado, 2005, Liu & Lehane 2020, Pucker et al. 2013) and pile foundations (Schneider et al. 2010) over the last two decades, but is yet to be explored in uplift capacity problems.

This paper explores the test results from an elaborate set of reported centrifuge experiments (vertical uplift tests) on circular, rectangular and strip anchors with companion cone penetrometer tests in different densities at various embedment depths, *g*-levels and OCR levels. The cone tip resistance (q_c) measured in the centrifuge were depth-corrected to remove the effect of shallow embedment. A correlation between plate anchor capacity and cone tip resistance is then developed using a regression analysis on the database of centrifuge anchor tests.

2 EXPERIMENTAL DATABASE DETAILS

The anchor database comprised of 91 uplift tests across 20 sand samples reported from two different centrifuge studies:

- Tests reported by Roy et al. (2021a,b) on strip, rectangular and circular plate anchors in silica sand of relative density, $R_D \sim 70\%$ and $R_D \sim 45\%$ (details in Table 1 and Table 2). These tests were conducted at gravitation accelerations ranging between 20*g* and 100*g*, and embedment ratios (*H*/*B*or *H*/*D*, where *H* is depth of the plate anchor, *B* is the anchor width and *D* is the anchor diameter) of 2 to 6 to investigate the behaviour of plate anchors under different stress levels (hence at different *g*) and load inclination. For the current study, only vertical uplift tests from the respective samples are included in the database.

DOI: 10.1201/9781003308829-163

- Tests reported by Hao et al. (2018) on circular plates and single helices in sand of R_D = 85-95% at 20*g*(details in Table 3) at anchor embedment ratios (*H*/*D*) in the range 2 to 10;

Table 1. Anchor database in loose sand (after Roy et al. 2021a).

Sample No., R_D (%) (and $\gamma(kN/m^3)$	Anchor code	*g*	*OCR*	*H*/*B* or *H*/*D*	Anchor factor, N_γ
D1, 76.72 (16.61)	ST_3	30	1	1.95	2.28
	ST_2	30	1	1.95	2.14
	ST_1	50	1	1.95	2.18
	R_2	30	1	2.00	3.49
	R_3	50	1	2.00	3.37
	R_1	100	1	2.05	3.38
D2, 73.5 (16.52)	ST_2	30	1	2.70	2.51
	ST_3	50	1	2.70	2.30
	R_2	30	1	2.70	3.73
	R_3	50	1	2.95	3.82
	R_1	100	1	2.68	3.25
	C_1	33.3	1	1.80	4.18
	C_2	66.6	1	1.80	3.43
D3, 75.28 (16.58)	ST_1	30	1	3.95	4.17
	ST_2	50	1	3.95	3.99
	R_3	30	1	4.00	7.11
	R_1	50	1	4.00	6.34
	R_2	100	1	4.00	6.15
	C_1	33.3	1	2.70	7.32
	C_2	66.6	1	2.70	6.68
D4, 75.14 (16.57)	ST_1	30	1	3.85	4.01
	ST_2	50	1	3.96	3.60
	R_1	30	1	3.81	5.98
	R_3	50	1	3.95	5.89
	R_2	100	1	3.85	5.59
	C_1	33.3	1	2.53	6.31
	C_2	66.6	1	2.57	6.12
D5, 69.53 (16.41)	R_4	20	1	1.80	2.96
	C_3	20	1	1.93	4.33
D6, 71.1 (16.45)	R_5	20	1	3.03	4.29
	C_3	20	1	2.90	8.28
D7, 74.35 (16.54)	R_4	20	1	3.77	6.55
D9, 78 (16.65)	C_5	30	1	5.94	14.46
	C_4	30	3	5.9	17.22
	C_7	30	5	5.87	18.21
	R_6	30	1	6.05	8.95
	R_5	30	1	5.8	8.58
	R_8	30	3	5.9	9.1
	R_7	30	5	5.93	9.2

These uplift tests involved anchors with different geometry (strip (ST) with aspect ratio 8:1, rectangular (R) with aspect ratio 2:1, circle (C), helix (H)) as listed in Tables 1-3 and Figure 1. All these tests were conducted in a fine sub-angular silica sand, commonly identified as the UWA Silica sand with properties as summarised in Table 4. The samples for the centrifuge tests were prepared using air pluviation technique and anchor testing setup can be found in the respective papers.

Table 2. Anchor database in loose sand (after Roy et al. 2021 a,b).

Sample No., R_D (%) (and $\gamma(kN/m^3)$	Anchor code	*g*	*OCR*	*H*/*B* or *H*/*D*	Anchor factor, N_γ
L1, 42.8 (15.68)	ST_2	30	1	1.75	1.31
	ST_3	50	1	1.75	1.33
	ST_1	100	1	1.75	1.26
	R_3	30	1	1.80	2.01
	R_2	50	1	1.80	1.90
	R_1	100	1	1.85	1.90
L2, 48.9 (15.84)	ST_2	30	1	2.75	1.56
	ST_1	50	1	2.75	1.60
	ST_3	100	1	2.75	1.56
	R_1	30	1	2.8	1.98
	R_2	20	1	2.75	2.82
	R_5	20	1	1.90	2.29
	R_4	33.3	1	1.83	1.72
	C_1	33.3	1	1.90	2.61
L3, 45.7 (15.76)	ST_2	30	1	3.60	2.38
	ST_3	50	1	3.85	2.35
	ST_1	75	1	3.70	2.25
	R_3	30	1	3.80	3.93
	R_2	50	1	3.80	3.86
	R_1	100	1	3.73	3.75
	C_1	33.3	1	2.53	4.70
	C_2	66.6	1	2.53	4.70
L4, 47.35 (15.8)	R_4	20	1	1.83	2.13
	C_3	20	1	1.90	2.39
L5, 47.37 (15.79)	R_4	20	1	2.87	3.33
	C_3	20	1	2.77	4.19
L6, 48.67 (15.83)	R_4	20	1	4.07	4.51
	C_3	20	1	3.90	6.04
L7, 50.21 (15.87)	C_6	30	1	5.78	9.73
	C_7	30	3	5.92	9.92
	C_5	30	5	5.95	12.27
	C_4	30	5	5.85	11.40
	R_8	30	1	5.78	6.46
	R_7	30	3	5.92	6.95
	R_6	30	5	5.93	8.97
	R_5	30	5	5.9	8.69

Companion cone penetrometer tests were also conducted in these reported studies at 20*g* using a 10 mm diameter cone penetrometer (d_{cone}).

Figure 2 presents q_c profiles measured across: (a) the 13 sand samples reported in Roy et al. (2021) at 20*g* performed at the start of testing, and (b) q_c profiles from the 13 sand samples in Hao et al. (2019). These q_c profiles are used to estimate the relative density (R_D) of the samples using a q_c - R_D relation proposed by Roy et al. (2019) for the UWA silica sands, that accounts for effective vertical stress(σ'_v), relative density and normalised penetration depth (z_m/d_{cone}):

$$q_c = C_0 P_a (\sigma'_v/P_a)^{C_1+C_3(1-f_D)+f_D\Delta C_{1oc}} (e)^{(C_2+f_D\Delta C_{2oc})R_D} \quad (1a)$$

$$f_D = \exp(-C_4(z_m/d_{cone})^{-C_5}) \quad (1b)$$

where the constants for UWA Silica sand were obtained as C_0 = 8.5, C_1 = 0.89, C_2 =3.3, C_3 = 0.36, C_4 = 1049.2 $R_D^{7.25}$, C_5 = 3.7 respectively. ΔC_{1-oc} and ΔC_{2-oc} are constants that account for the decreased compressibility of the sands under OC condition, the details of which are explained in Roy et al. (2019). It is worth noting that the effect of shallow embedment on $q_c$for centrifuge CPTs are incorporated through a varying depth factor (f_D) in Equation 1. Using Equation 1, relative density at the anchor locations was back-analysed as R_D = 41 – 51% for the loose sand and R_D = 69 – 76% in the dense sand reported by Roy et al. (2021a). For the tests reported by Hao et al (2019) on circular plates, the R_D was ~ 85 - 96%.

Table 3. Anchor database in very dense sand at 20g and OCR = 1 (after Hao et al., 2019).

Relative density (%) (unit weight) (kN/m^3)	Anchor code	*H/D*	q_a (kPa)	N_γ
96.2 (17.07)	H	3	182.29	8.9
86.7 (16.87)	H	4	340.12	12.6
86.4 (16.86)	H	6	861.68	21.3
96.2(17.07)	H	6	966.73	23.6
90 (16.94)	H	7.5	1285.68	25.3
86.4 (16.86)	H	8	1407.82	26.1
96.4 (17.07)	H	8	1731.80	31.7
88.8 (16.91)	H	9	1991.16	32.7
96.1 (17.07)	H	9	2156.46	35.1
96.2 (17.07)	H	9	2070.69	33.7
96.4 (17.07)	H	10	2465.23	36.1
90 (16.94)	H	10.5	2169.90	30.5
86.7 (16.87)	H	2	78.28	5.8
85.8 (16.84)	C	3	181.87	9.0
85.8 (16.84)	C	6	860.86	21.3
85.8 (16.84)	C	9	1879.34	31.0

For anchor tests conducted at different *g*-levels or OCRs within the same sample (see samples D1-D7, D9 in Table 1 and L1-L7 in Table 2), a q_c profile at the respective *g*-level or OCR was required to generate the correlate to anchor capacity. However, CPT tests at all *g*-levels as those of the anchor tests were not possible due to the space constraints in the strongboxes; as such Equation (1) was subsequently used in such cases to establish the respective q_c profile. The validity of such an approach is confirmed by the good agreement between the measured and simulated q_c - z_m/d_{cone} profiles using Equation (1) at two different R_D and *g*-levels in a separate CPT study as shown in Figure 3.

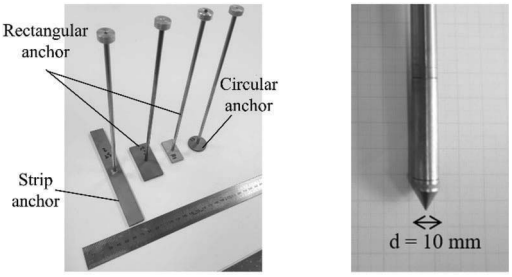

Figure 1. Model plate anchors and piezocone (after Roy et al. 2021a, b).

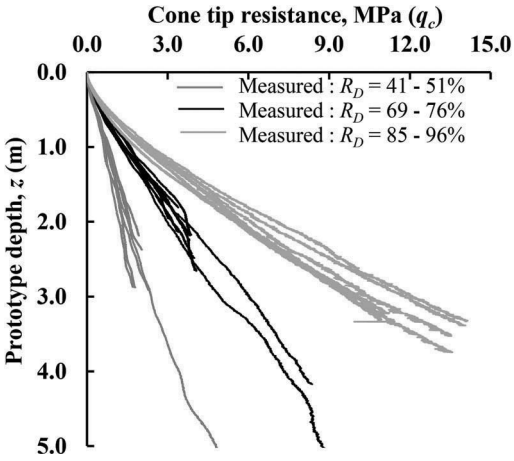

Figure 2. Measured q_c profiles in loose, dense (Roy et al., 2021a) and very dense sand (Hao et al., 2019).

Table 4. Physical properties of UWA silica sand.

Soil properties	UWA Silica sand
Angularity	Sub-rounded to sub-angular
Maximum void ratio[a]	0.789
Minimum void ratio[a]	0.512
Specific gravity[b]	2.67
Uniformity coefficient (*U*)	1.73
Mean particle size (d_{50})	0.2 mm

a Maximum and minimum void ratios calculated as per AS 1289.5.5.1

b Specific gravity calculated as per AS 1289.3.5.1

3 ESTABLISHING N_Γ - q_c CORRELATIONS

3.1 *Anchor capacity factor*

The mobilised peak anchor capacity (q_a) in this paper is reported in dimensionless form as peak anchor factor ($N_\gamma = q_a/\sigma'_{vo}$, where σ'_{vo} is the effective overburden stress). The q_a and N_γ for each anchor test is tabulated in Tables 1-3. The N_γ is typically attained within normalized displacement (δ/B or δ/D) of 15% in medium dense (R_D = 48%) and 7-12% % in dense sand (R_D = 70%), as reported in Roy et al. (2021a,b). At a given H/B, the highest N_γ is observed from circular plates whereas the least is observed from strip anchors.

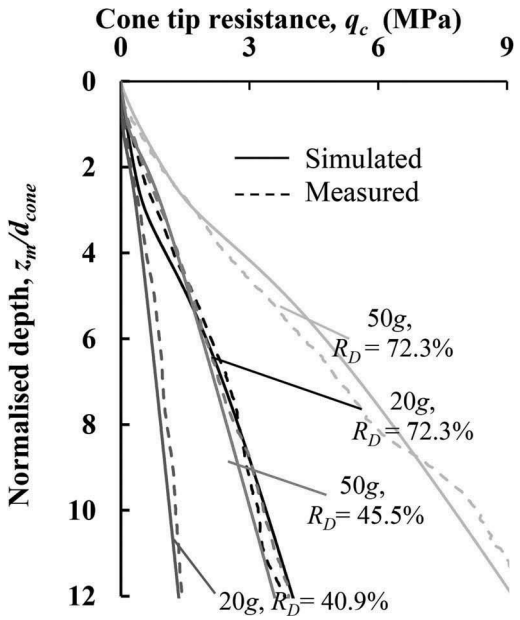

Figure 3. Comparison of measured and simulated q_c - z_m/d_{cone} profiles at different R_D and g-levels.

3.2 *Correcting q_c for shallow embedment effects*

The q_c profiles from centrifuge samples undergo shallow penetration and need to be corrected for effects of shallow embedment (Bolton *et al.* 1999). For example, if the results for a prototype anchor having D = 0.6 m at H/D of 2 was to be simulated, a model anchor plate with diameter of 30 mm (as reported in the database) would have to be embedded at a sample depth of 60 mm at 20g. With centrifuge penetrometers having d_{cone} = 10 mm, the anchor placement depth would be located within a penetrating distance of $6d_{cone}$, resulting in a shallow failure mechanism for the penetrometer. For corresponding prototype anchors having D = 0.6 m, it would have to be embedded at a depth of 1.2 m in field (for H/D = 2); a penetrometer in such conditions would have penetrated by ~$33d_{cone}$ (considering a standard cone diameter of 35.8 mm) to reach embedded depth for the anchor, resulting in a deep failure mechanism. As per reported studies by Bolton et al. (1999) and Liu & Lehane (2020), the critical normalised depth governing the transition from shallow to a deep mechanism for a cone penetration test usually ranges between 5 and 15. So, cone profiles from centrifuge samples would produce a smaller q_c value at shallow depths than the corresponding prototype samples at similar stress and density levels. Hence, correction is necessary to obtain an equivalent q_c value under the effect of similar stress and density levels but independent of penetrating distance. This can be readily worked out using the correlations by use of depth factor f_d = 1.

The depth-corrected q_c profiles simulated using f_d = 1 in Equation (1) is shown in Figure 4 for two different densities at two different stress levels. These profiles show that the effect of depth correction on q_c is more pronounced as the g-level and the R_D increases. For the measured (uncorrected) centrifuge $q_c$profiles in Figure 4, a shallow failure mechanism results in an increased concave upwards curvature at the shallower penetration depths. In contrast, the simulated (depth-corrected) profiles are convex-shaped at the shallow penetration depths. The simulated and measured profiles tend to merge with each other at z/d_{cone} value greater than 8.

3.3 *Obtaining average q_c values*

The anchor tests reported in Table 1-3 were conducted at stress levels ranging from 20g to 100g. In order to obtain a correlation between N_γ and q_c, a representative q_c value in the influencing domain was necessary at the corresponding g level of the anchor test. Numerical studies have confirmed that (Al Hakeem and Aubeny, 2019, Hao et al. 2014), for plate anchor uplift under drained conditions, the failure mechanism significantly mobilises a soil on top of the anchor plate up to a distance of 2D or 2B. Based on this evidence, a representative q_c value (termed as $q_{c,avg}$) was taken as the average over a distance of 2D or 2B over the top of the anchor using the depth-corrected simulated q_c profiles obtained by correlations in Equation 1. This zone encompasses the distance required to mobilise peak N_γ for all anchor types and embedment ratios.

3.4 *Correlation for anchors*

Figure 5 presents the average cone tip resistance ($q_{c,avg}$) vs. mobilised peak anchor capacity (q_a) data at all g levels for circular anchor. The data shows q_a linearly with an increase in $q_{c,avg}$ for all anchor types. However, at a particular value of $q_{c,avg}$, q_a values from loose sand are observed to higher than those in dense sand. Now, in order to inter-compare q_a at similar $q_{c,avg}$ values in loose and dense sand, an anchor would have to be located at a much deeper depth (or higher σ'_v) for the loose sand than for the dense sand. This suggests that there appears to be a significant contribution of σ'_v in governing peak N_γ. This hints that a stress normalised $q_{c,avg}$ value would be necessary to reliable correlation.

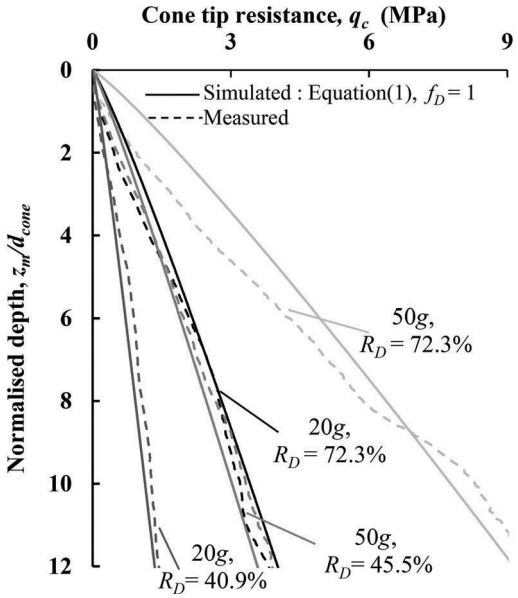

Figure 4. Comparison of measured cone profiles and simulated cone profiles using f_D = 1 at different g-levels in loose and dense sand.

In order to capture the effects of stress on the penetration resistance, Sharp et al. (2010) suggested the use of a normalised tip resistance term q_{c1N}:

$$q_{c1N} = (q_c/P_a)(P_a/\sigma'_v)^m, \qquad (2)$$

where P_a is the atmospheric pressure, σ'_v is the effective overburden stress and m is a stress exponent term ranging from 0.3 to 0.8 that better accounts for the effects of σ'_v for a given problem. Trial iterations with using m = 1 across all densities (i.e. without using any R_D dependent normalisation), showed that insufficient overlap across all datasets, thus hindering the development of a unique correlation. This suggested that a density dependent m value needs to be used to ensure sufficient overlap between the datasets.

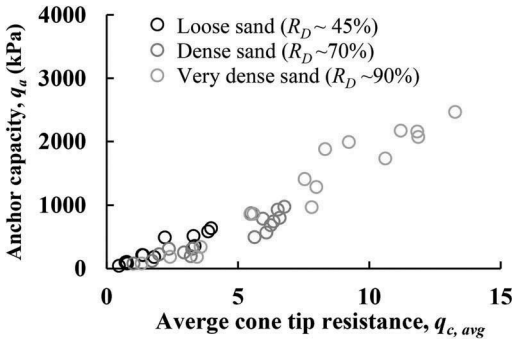

Figure 5. Variation of peak anchor capacity with average cone tip resistance in loose and dense sands for circular anchors.

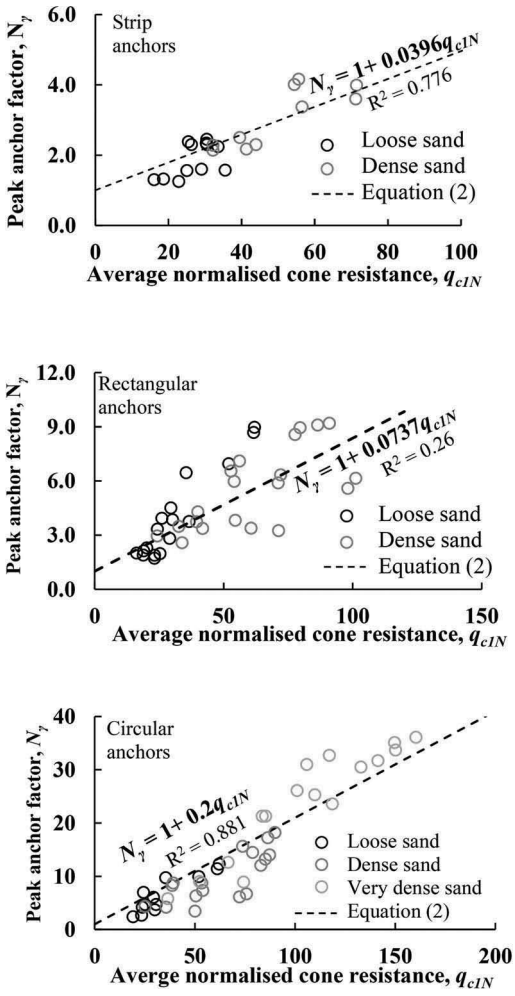

Figure 6. Correlation of N_γ with q_{c1N} in loose and dense sand for (a) strip anchors, (b) rectangular anchors and (c) circular anchors.

The value of m was therefore evaluated using an optimisation routine to produce the greatest overlap in loose and dense sand data by a relative shift in the abscissa of the N_γ - q_{c1N} plot. This was achieved iteratively resulting in a value of m = 0.6 in loose sands (R_D ~45%), 0.4 in dense sands (R_D ~70%) and 0.39 in very dense sands (R_D ~90%). More anchor experimental data at R_D < 40% would be required to draw an unambiguous conclusion on the precise values of m in very loose sand. In absence of such data, it is assumed that m would take an upper bound of 0.8 at very low R_D values, therefore the exponent m used to obtain q_{c1N} can be expressed as:

$$m = 0.41(R_D(\%)/100)^{-0.24} \qquad (3)$$

Applying the optimized m in Equation (2), the correlation between q_{c1N} and $N_\gamma$is established as shown in Figure 6 and presented in Equation (4):

$$N_\gamma = 1 + f_u\, q_{c1N} \tag{4}$$

where f_u is a coefficient dependent on anchor shape and is equal to 0.0396, 0.0784 and 0.2 for strip, rectangular and circular plates respectively. The R^2 values for the respective correlations for strip, rectangular and circular plate anchors are 0.776, 0.26 and 0.881 respectively. The significantly lower R^2 of 0.26 for the rectangular anchors is due to greater scatter in the experimental dataset at lower q_{c1N} levels and suggests that more experimental data would be required to obtain a reliable correlation. The f_u values also indicate that the anchor capacity increases in the order of strip, rectangular and circular anchors, which agree with existing studies (e.g. Murray and Geddes 1987).

4 CONCLUSIONS

A correlation between anchor capacity factor (N_γ) and normalized cone tip resistance (q_{c1N}) has been established based on a collected database of centrifuge tests on strip, rectangular and circular anchors at varying g-levels in loose and dense sands. The centrifuge cone profiles were depth-corrected to remove the effect of shallow embedment and make them inter-comparable with prototype tests. The results indicated that a varying stress exponent factor is necessary to account for the effect of overburden stress in loose and dense sands and to establish a unique correlation. It is desired to validate the proposed N_γ -q_{c1N} correlation using field anchor and companion CPT data. The results can also be used to readily compute anchor capacity through CPT profiles when the soil fabric has been disturbed due to installation effects, which is a distinct advantage when compared to other methods relying on in-situ inputs of density and friction angles.

ACKNOWLEDGEMENTS

The authors acknowledge the financial support from the Australian Research Council Discovery Grant Scheme DP190100914.

REFERENCES

Been, K., Jefferies, M. G. & Hachey, J. 1999. The critical state of sands. *Géotechnique* 41(3): 365–381. doi: 10.1680/geot.1991.41.3.365.

Bolton, M. D., Gui, M.W., Garnier, J., Corte, J.F., Bagge, G., Laue, J. & Renzi, R. 1999. Centrifuge cone penetration tests in sand. *Géotechnique* 49(4): 543–552. doi: 10.1680/geot.1999.49.4.543.

Gajo, A. & Wood, D. M. 1999. A kinematic hardening constitutive model for sands: the multiaxial formulation. *International Journal for Numerical and Analytical Methods in Geomechanics* 23: 925–965.

Al Hakeem, N. & Aubeny, C. 2019. Numerical Investigation of Uplift Behavior of Circular Plate Anchors in Uniform Sand. *Journal of Geotechnical and Geoenvironmental Engineering* 145(9): doi: 10.1061/(asce)gt.1943-5606.0002083.

Hao, D., Wang, D., O' Loughlin, C.D. & Gaudin, C. 2019. Tensile monotonic capacity of helical anchors in sand: interaction between helices. *Canadian Geotechnical Journal* 56(10):1534–1543. doi: 10.1139/cgj-2018-0202.

Hao, D., Fu, S. & Rong, C. 2014. Numerical Analysis of Uplift Capacity of Circular Plate Anchor in Sand. *Journal of geotechnical engineering* 19: 18947–18961.

Lee, J. & Salgado, R. 2005. Estimation of Bearing Capacity of Circular Footings on Sands Based on Cone Penetration Test. *Journal of Geotechnical and Geoenvironmental Engineering* 131(4): 442–452.

Liu, Q. & Lehane, B. M. 2020. A centrifuge investigation of the relationship between the vertical response of footings on sand and CPT end resistance. *Géotechnique* 71 (5):1–11. doi: 10.1680/jgeot.19.p.253.

Murray E.J. & Geddes, J.D. 1987. Uplift of anchor plates in sand. *Journal of Geotechnical and Geoenvironmental Engineering* 113(3): 202–215.

Pucker, T., Bienen, B. & Henke, S. 2013. CPT based prediction of foundation penetration in siliceous sand. *Applied Ocean Research* 41: 9–18. doi: 10.1016/j.apor.2013.01.005.

Roy, A., Chow, S., O' Loughlin, C.D. & Randolph, M.F. 2021a. Towards a simple and reliable method for calculating uplift capacity of plate anchors in sand. *Canadian Geotechnical Journal* 58(9): 1314–1333. doi: 10.1139/cgj-2020-0280.

Roy, A., O' Loughlin, C.D., Chow, S. & Randolph, M.F. 2021b. Inclined loading of horizontal plate anchors in sand. *Géotechnique:* doi: 10.1680/jgeot.20.P.119

Schneider, J. A., Xu, X. & Lehane, B. M. 2010. End bearing formulation for CPT based driven pile design methods in siliceous sands. *2nd International Symposium on Cone Penetration Testing* 3(May): 8.

Sharp, M. K., Dobry, R. & Phillips, R. 2010. CPT-Based Evaluation of Liquefaction and Lateral Spreading in Centrifuge. *Journal of Geotechnical and Geoenvironmental Engineering* 136(10):1334–1346. doi: 10.1061/(ASCE)GT.1943-5606.0000338.